

# X-RAY INDUCED CYTOTOXICITY OF AQUEOUS COLLOIDAL SOLUTIONS OF UV-C LUMINESCENT La<sub>1-x</sub>Pr<sub>x</sub>PO<sub>4</sub> NANOPARTICLES

Shaidulin A.T.<sup>1,2</sup>, Orlovskaya E.O.<sup>1</sup>, Uvarov O.V.<sup>1</sup>, Silaev G.O.<sup>2,3</sup>, Skopin P.I.<sup>4</sup>, Gololobova I.A.<sup>4</sup>, Al-khadj Aioub A.M.M.<sup>4</sup>, Yakobson D.E.<sup>4</sup>, Chernobay R.A.<sup>4</sup>, Vainer Y.G.<sup>3</sup>, Orlovskii Yu.V.<sup>1</sup>, Makhov V.N.<sup>5</sup>

- <sup>1</sup> Prokhorov General Physics Institute of the Russian Academy of Sciences Moscow, Russia
- <sup>2</sup> Higher School of Economics National Research University, Moscow, Russia
- <sup>3</sup> Institute of Spectroscopy of the Russian Academy of Sciences, Moscow, Russia
- <sup>4</sup> National Research Ogarev Mordovia State University, Saransk, Russia
- <sup>5</sup> P.N. Lebedev Physical Institute of the Russian Academy of Sciences, Moscow, Russia

#### **Abstract**

The use of UV-C radiation for the treatment of tumors is a stand-alone therapeutic intervention that can induce cellular apoptosis and is independent of photosensitizer or oxygen concentration in tumor. To explore the potential of using X-ray excited UV-C luminescent nanoparticles as a basis for creating drugs to improve radiation therapy, two colloidal solutions of monoclinic La<sub>1-x</sub>Pr<sub>x</sub>PO<sub>4</sub> nanoparticles with different morphologies of large nanofibers (x = 0.02) or small nanorods (x = 0.05) were prepared using a microwave-assisted hydrothermal method. Comparison of X-ray excited UV-C luminescence of colloidal solutions showed approximately 6.3 times higher brightness for larger nanoparticles. The intrinsic and X-ray-induced cytotoxicity of the prepared colloidal solutions on the viability of cancerous Mh22a and healthy L929 cell cultures were studied using MTT assay and fluorescence microscopy. Fluorescence microscopy showed differences in the types of cell death (apoptosis or necrosis) after incubation with nanofiber or nanorod samples. X-ray irradiation was performed in two modes with different voltage on the X-ray tube (50 and 80 kV) and the same radiation dose (8 Gy). Groups of cells incubated with nanoparticles and irradiated with 50 kV mode showed greater death rate. According to MTT analysis, irradiation of cells incubated with La<sub>0.98</sub>Pr<sub>0.02</sub>PO<sub>4</sub> nanofibers at a concentration of 2 mg/mL reduced survival by 20-30%, and at the same time, according to fluorescence microscopy data, the number of cells undergoing apoptosis exceeded the number of cells that died through necrosis and reached 50-70%. Quantitative analysis of the relative number of dead cells caused by X-ray-induced cytotoxicity of La<sub>0.98</sub>Pr<sub>0.02</sub>PO<sub>4</sub> nanorods did not reveal statistically significant results in reducing cell viability.

**Key words:** UV-C luminescence, X-ray excited optical luminescence, aqueous colloidal solution of nanocrystals, X-ray induced cytotoxicity, *in vitro*, fluorescence microscopy, apoptosis.

Contacts: Shaidulin A.T., e-mail: shatarte@yandex.ru

**For citations**: Shaidulin A.T., Orlovskaya E.O., Uvarov O.V., Silaev G.O., Skopin P.I., Gololobova I.A., Al-khadj Aioub A.M.M., Yakobson D.E., Chernobay R.A., Vainer Y.G., Orlovskii Yu.V, Makhov V.N. Experimental studies X-ray induced cytotoxicity of aqueous colloidal solutions of UV-C luminescent La<sub>1...</sub>Pr<sub>.</sub>PO<sub>4</sub> nanoparticles, *Biomedical Photonics*, 2025, vol. 14, no. 3, pp. 14–23. doi: 10.24931/2413–9432–2025–14-3–14–23

# РЕНТГЕН-ИНДУЦИРОВАННАЯ ЦИТОТОКСИЧНОСТЬ ВОДНЫХ РАСТВОРОВ УФ-С РЕНТГЕНОЛЮМИНЕСЦЕНТНЫХ НАНОЧАСТИЦ $La_{1-x}Pr_{x}PO_{x}$

А.Т. Шайдулин<sup>1,2</sup>, Е.О. Орловская<sup>1</sup>, О.В. Уваров<sup>1</sup>, Г.О. Силаев<sup>2,3</sup>, П.И. Скопин<sup>4</sup>, И.А. Гололобова<sup>4</sup>, Аль-хадж Аюб А.М.М.<sup>4</sup>, Д.Э. Якобсон<sup>4</sup>, Р.А. Чернобай<sup>4</sup>, Ю.Г. Вайнер<sup>3</sup>, Ю.В. Орловский<sup>1</sup>, В.Н. Махов<sup>5</sup>

<sup>1</sup>Институт общей физики им. А.М. Прохорова Российской академии наук, Москва, Россия <sup>2</sup>Национальный исследовательский университет «Высшая школа экономики», Москва, Россия

<sup>3</sup>Институт спектроскопии Российской академии наук, Москва, Россия

<sup>4</sup>Национальный исследовательский Мордовский государственный университет им. Н.П. Огарёва, Саранск, Россия

 $^5$ Физический институт им. П.Н. Лебедева Российской академии наук, Москва, Россия



## Резюме

Использование УФ-С излучения является отдельно стоящим терапевтическим воздействием на раковые опухоли, которое способно вызывать клеточный апоптоз и не зависит от фотосенсибилизатора или концентрации кислорода в опухоли. Для исследования потенциала использования наночастиц, способных к рентгенолюминесценции в УФ-С области, в качестве основы для создания препарата, направленного на улучшение лучевой терапии, гидротермально-микроволновым методом были приготовлены два коллоидных раствора наночастиц моноклинного  $La_{1-x}Pr_xPO_4$  с морфологиями крупных нановолокон (x = 0,02) или мелких наностержней (x = 0,05). Сравнение рентгенолюминесценции в УФ-С области коллоиных растворов показало в 6,3 раз превосходящую яркость для более крупных наночастиц. Собственная и рентген-индуцированная цитотоксичность коллоидных растворов на культуре опухолевых клеток Mh22a и культуре клеток L929 были исследованы при помощи МТТ анализа и флуоресцентной микроскопии. Флуоресцентная микроскопия выявила различия в форме клеточной смерти (апоптоз или некроз) после инкубации клеток с образцами нановолокон или наностержней. Облучение рентгеном проводили в двух режимах с различным напряжением на рентгеновской трубке (50 или 80 кВ) и с одинаковой дозой облучения (8 Гр). Группы клеток, инкубированные с крупными наночастицами и облученные в режиме 50 кВ, показали более высокие показатели гибели. Согласно МТТ анализу, облучение клеток, инкубированных с нановолокнами  $La_{0.98}Pr_{0.07}PO_4$  с концентрацией 2 мг/мл, снизило выживаемость на 20-30%, и одновременно по данным флуоресцентной микроскопии, количество клеток, находящихся в апоптозе, превысило число клеток погибших путем некроза и достигло 50-70%. Количественный анализ относительного числа погибших клеток, исследованных на влияние рентген-индуцированной цитотоксичности наностержей  $La_{0.95}Pr_{0.05}PO_{4}$ , не выявил достоверных результатов по снижению жизнеспособности клеток.

**Ключевые слова**: УФ-С люминесценция, рентгенолюминесценция, водный коллоидный раствор нанокристаллов, рентген-индуцированная цитотоксичность, *in vitro*, флуоресцентная микроскопия, апоптоз.

Контакты: A.T. Шайдулин, e-mail: shatarte@yandex.ru

**Для цитирования:** Шайдулин А.Т., Орловская Е.О., Уваров О.В., Силаев Г.О., Скопин П.И., Гололобова И.А., Аль-хадж Аюб А.М.М., Якобсон Д.Э., Чернобай Р.А., Вайнер Ю.Г., Орловский Ю.В., Махов В.Н. Рентген-индуцированная цитотоксичность водных растворов УФ-С рентгенолюминесцентных наночастиц  $La_1$ ,  $Pr_2$   $PO_4$  // Biomedical Photonics. − 2025. − T. 14,  $N^2$  3. − C. 14−23. doi: 10.24931/2413−9432−2025−14−3−14−23

#### Introduction

A separate mechanism of action on cancer tumors without the use of a photosensitizer (but not excluding it) may be the use of nanoparticles (NPs) exhibiting X-ray excited optical luminescence in the UV-C (200-280 nm) region. It is known that UV-C quanta have the ability to initiate cell apoptosis due to direct photochemical reactions in DNA molecules [1]. This property should help reduce tissue necrosis, which should facilitate the body's recovery. Since body tissues strongly absorb UV-C radiation, to affect deep-seated solid tumors it is necessary to create a localized source of UV-C quanta, which can be excited by X-ray irradiation, which easily penetrates biological tissue. To the best of our knowledge, only one research group has tested the effect of nanoparticles (NPs) capable of X-ray-excited optical luminescence in the UV-C spectral range (lutetium phosphate NPs doped with Pr<sup>3+</sup> and Nd<sup>3+</sup> ions) on the deactivation of cancer cells [2-6]. The most significant effects of the combined action of X-ray-excited UV-C fluorescent nanoparticles and X-ray irradiation were demonstrated in vitro in [2, 6]. An increase in the efficiency of radiation exposure under hypoxic conditions [2] and the possibility of strong inhibition of cancer spheroid growth as a result of apoptosis, cell cycle arrest and necrosis [6] were demonstrated.

However, high intensity UV-C radiation can also be observed in other suitable crystalline matrices doped with Pr<sup>3+</sup> or Nd<sup>3+</sup> ions due to the presence of interconfigurational electronic transitions in these ions from the excited electron configuration 4f<sup>n-1</sup>5d<sup>1</sup>

to the ground electron configuration  $4f^n$  (n = 2 and 3, respectively). Among them is LaPO, nanocrystals with monazite structure (m-LaPO<sub>4</sub>, monoclinic system, P2<sub>1</sub>/n) doped with Pr<sup>3+</sup> ions, which also exhibit strong emission in the UV-C range (220–280 nm) due to  $4f^15d^1 \rightarrow {}^3H_{4.5.6}$ <sup>3</sup>F<sub>2</sub> transitions in Pr<sup>3+</sup> ions under high-energy excitation [7-12]. Since La<sup>3+</sup> and Pr<sup>3+</sup> ions have close ionic radii and form the same phosphate crystal structure, a higher degree of substitution of cations with lower structural defects can be expected. In addition, the  $4f^15d^1 \rightarrow {}^3H_e$ transition in Pr3+ ions has an intensity maximum in the spectral range of 256 nm [7], which practically coincides with the absorption maximum of DNA [3]. Based on this, the aim of this work was to conduct an in vitro study of the intrinsic and X-ray-induced cytotoxicity of aqueous colloidal solutions of m-La,\_Pr,PO, NPs.

Two colloidal solutions of La<sub>1-x</sub>Pr<sub>x</sub>PO<sub>4</sub> NPs with different morphologies were synthesized by the hydrothermal microwave-assisted method: nanofibers (La<sub>0.98</sub>Pr<sub>0.02</sub>PO<sub>4</sub>) with NPs length up to 600 nm and diameter up to 15 nm and nanorods (La<sub>0.95</sub>Pr<sub>0.05</sub>PO<sub>4</sub>) with length up to 80 nm and diameter up to 10 nm. X-ray excited optical luminescence spectroscopy in the UV-C region of the obtained samples in the form of colloidal solutions using a highly sensitive N<sub>2</sub>-cooled CCD camera designed for the UV range. The intrinsic cytotoxicity and X-ray-induced cytotoxicity of the obtained colloidal solutions of La<sub>1-x</sub>Pr<sub>x</sub>PO<sub>4</sub> NPs with different morphologies was investigated *in vitro* by MTT assay. The X-ray-induced cytotoxicity studies were conducted using therapeutic X-ray radiation operating



ORIGINAL ARTICLES

in two different modes of the X-ray tube (accelerating voltage 50 and 80 kV) and a total dose of 8 Gy. Groups of cells irradiated with X-rays under the same conditions without NPs, as well as irradiated with a UV lamp, were used as controls. The nature of cell death of the control groups of cells was studied using double staining of cells and subsequent fluorescence microscopy.

#### **Materials and Methods**

Synthesis of colloidal solutions of La, Pr, PO, nanoparticles with different morphologies

The initial chemical reagents used in the synthesis without further purification include: Pr(NO<sub>2</sub>)<sub>2</sub>·6H<sub>2</sub>O (Aldrich, 99.9% purity), La(NO<sub>3</sub>)<sub>3</sub>·6H<sub>2</sub>O (Aldrich, 99.999% purity), K<sub>2</sub>HPO<sub>2</sub>·3H<sub>2</sub>O (RusKhim, analytical grade), tartaric acid (hps, analytical grade), 25% agueous solution of NH, OH (SigmaTek, analytical grade). Throughout all syntheses, deionized (DI) water (type I) from a water deionizer Crystal EX-1001 (Adrona) was used.

La<sub>0.98</sub>Pr<sub>0.02</sub>PO<sub>4</sub> sample consisting of nanofibers (NPs length & diameter not larger than 600 & 15 nm, respectively) was prepared with 0.5 mmol of REIs (0.49 mmol of La(NO<sub>3</sub>)<sub>3</sub>·6H<sub>2</sub>O and 0.01 mmol of Pr(NO<sub>3</sub>)<sub>3</sub>·6H<sub>2</sub>O) and an anion excess ratio of K<sub>2</sub>HPO<sub>4</sub> equal to 1.25. The solution of REIs (10 mL) was continuously supplied (0.4 mL/min) using a syringe pump directly into solution containing excess K<sub>2</sub>HPO<sub>4</sub> (15 mL) with constant stirring. The formed cloudy solution of gel was diluted with DI water to a volume of 50 mL (resulting pH = 5), transferred to a 100 ml autoclave (DAK-100), sealed and treated at 200 °C for 2 hours under microwave-hydrothermal conditions using a speedwave XPERT (Berghof Products+Instruments GmbH) laboratory device with two magnetrons (2.45 GHz, 2 kW maximum output power). After hydrothermal treatment, the sediment from the bottom of autoclave was washed twice with a weak solution of HNO, and once with DI water (80 mL each time) using a centrifugationredispersion using a centrifuge (14800 rf, 15 min). After the third washing, the suspension ring was redispersed in 5 mL of DI water forming a turbid translucent solution (pH of the final colloidal solution was 5.3). La<sub>0.95</sub>Pr<sub>0.05</sub>PO<sub>4</sub> sample consisting of nanorods (NPs length & diameter not larger than 80 & 10 nm, respectively) was prepared with 0.5 mmol of REIs (0.475 mmol of La(NO<sub>3</sub>)<sub>3</sub>·6H<sub>2</sub>O and 0.025 mmol of Pr(NO<sub>3</sub>)<sub>3</sub>·6H<sub>2</sub>O) and anion excess ratio of K<sub>2</sub>HPO<sub>4</sub> equal to 2. The pH of the REIs solution was adjusted to pH = 8 using alkaline solution of ammonium tartrate and NH<sub>4</sub>OH, which acted as a weak complexing agent, preventing, the formation of hydroxides. After hydrothermal-microwave treatment (200°C, 2 h), the precipitate was washed twice with DI water, then with a weak NH,OH solution using the centrifugationredispersion process, followed by redispersion in 5 mL of DI water, resulting in a transparent colloidal solution (pH of the final colloidal solution was 7.5).

Transmission electron microscopy

TEM images of NPs were obtained on a Zeiss Libra 200 FT HR microscope under accelerating voltage of 200 kV. The colloids were highly diluted and applied onto a TEM grid and dried in vacuum for several hours. ImageJ software was used to measure sizes of individual nanocrystals by approximating the length and diameter of the observed TEM projections with straight perpendicular lines.

X-ray excited optical luminescence spectroscopy of colloidal solutions

X-ray excitation of the studied samples in the form of a colloidal solution was performed using X-ray tube MOX-HPC 150W 60kV equipped with tungsten anode (Moxtek). The X-ray excited optical luminescence in the UV-C spectral region was recorded using a HORIBA iHR-550 Imaging spectrometer (Horiba Scientific) with a diffraction grating of 1800 grooves/mm and a N<sub>2</sub>-cooled PyLoN:2KBUV CCD camera (Princeton Instruments) designed for the UV spectral range. A self-made objective based on two planoconvex lenses made of MgF<sub>2</sub> with a light spot diameter of 35 mm and a focus of 70 mm was used to collect the UV-C light. Colloidal solutions were applied to a polytetrafluoroethylene (PTFE) substrate as a 0.2 mL drop with NPs concentration of 7 mg/mL. The operating mode of the X-ray tube for both types of colloidal solutions was: accelerating voltage: 30 kV; anode current: 2.5 mA; exposure time: 60 s.

Cell strains

The research in the work was carried out on the mouse cell cultures of Mh22a hepatoma (Biolot) and L929 fibroblasts (National Research Center of Epidemiology and Microbiology). The cells were grown in flasks with DMEM culture medium (Servicebio) supplemented with 10% fetal bovine serum (FBS, Biosera) and antibiotics: 100 μg/mL penicillin, 100 μg/mL streptomycin (Paneco). The incubation of cells was done in cell incubator (Thermoscientific Midi40), and conditions were standard: 5% CO<sub>2</sub>, temperature and humidity of the medium 37°C and 5%, respectively. Cell counting was performed using 0.4% trypan blue solution (Paneco) in a Goryaev chamber.

Design of the experimental in vitro study

The cytotoxicity of La<sub>1-x</sub>Pr<sub>x</sub>PO<sub>4</sub> NPs was determined using the photocolorimetric MTT assay in accordance with the international protocol ISO SO 10993-5:2009 "Tests for In Vitro Cytotoxicity". Cell cultures were seeded at 5000 cells per well and incubated in a 96-well plate for 24 hours under standard conditions. Then the culture medium was removed and replaced with a new medium (DMEM with 1% FBS) containing NPs at a concentration of 0.0625, 0.125, 0.25, 0.5, 1, 2, 4 mg/mL (n=3). The viability of the cell cultures was determined after 24 hours. After the time had elapsed, the medium with the studied samples was removed, the wells were washed twice with phosphate buffer, then 100 µl of fresh medium (DMEM with 1% FBS) and 10 µl of MTT solution (3-(4,5-dimethylthiazol-2-yl)-2,5-diphenyl) tetrazolium bromide) at a concentration

of 5 mg/mL were added to each well. After 3.5 hours of incubation, the formed formazan crystals were dissolved using a DMSO solution, which was added in 150  $\mu$ l to each well. The plates were then placed in a thermostatic shaker (ELMI ST-3L) for 20 min at 37°C, 400 rpm. Optical density was measured using a Varioscan Lux multimodal reader (Thermoscientific) at an analytical wavelength of 570 nm versus a reference wavelength of 650 nm. Cell viability was assessed by the ratio of the optical density of the samples to the optical density of the control cells (untreated cells incubated without additional components or external influences), expressed as a percentage.

The effect of La<sub>1-x</sub>Pr<sub>x</sub>PO<sub>4</sub> NPs on the viability of Mh22a and L929 cell cultures irradiated with X-rays was studied using a Terad 200 X-ray therapy apparatus (LINEV ADANI) equipped with a tungsten anode. The study was conducted in two modes: 1) the accelerating voltage, anode current, and Al filter thickness: 50 kV, 20 mA, and 0.5 mm, respectively; 2) the accelerating voltage, anode current, and Al filter thickness: 80 kV, 15 mA, and 2 mm, respectively. In both modes, the irradiation dose was 8 Gray. La<sub>1-x</sub>Pr<sub>x</sub>PO<sub>4</sub> NPs at concentrations of 1 and 2 mg/mL (n=8) were incubated with Mh22a and L929 cell culture in a 96-well plate (5000 cells per well) for 12 hours. Cell viability was determined using the MTT assay 24 h after X-ray exposure according to the protocol described above.

The type of cytotoxicity after incubation of Mh22a and L929 cells with NPs and exposure to X-ray radiation was determined using the double staining method and fluorescence microscopy using an Axio Zeiss Imager A1 microscope (Carl Zeiss Jena). As an additional control, groups of Mh22a and L929 cells were irradiated with a UV lamp at 60 J/cm² for 8 min. Selected control groups of Mh22a and L929 cells were stained with a mixture of acridine orange (AO) and propidium iodide (PI) dyes and then analyzed according to the protocol [13]. AO penetrates living, apoptotic and dead cells and stains their nuclei green or orange. In the case of intact DNA, AO fluoresces green. In early apoptosis, with the initial chromatin condensation, AO fluorescence appears yellow-green, and with DNA fragmentation, it appears

orange. In the late stage of apoptosis, when condensed chromatin disintegrates and the nucleus fragments, the binding of AO to DNA fragments weakens and the cell is stained green again. Propidium iodide penetrates only into dead cells with a damaged membrane (necrotic or late apoptotic) and stains the nucleus red. Thus, separation of cells into groups of viable, apoptotic, and necrotic cells was performed based on the morphological appearance of the cells. Viable cells (VC) were determined by uniform green staining and a fusiform shape. The early apoptotic cells (AC) were determined by cell shrinkage and DNA fragmentation which appears as bright orange staining of nuclei, with the borders of the nuclei clearly visible. The late AC were determined by nuclear disintegration, resulting in cells with bright green nuclei and cytoplasm. Additionally, signs of AC included rounding of cells and small fragments around them – apoptotic bodies. Necrotic cells (NC) were determined by a damaged membrane, a red or red-orange nucleus and cytoplasm, and a rounded shape. The cells that have completed the apoptotic cycle are then poorly distinguishable from necrotic cells, and therefore they were also included in the group of NC. Differentiation of the VC, AC and NC was performed by counting at least 100 cells in each independent group. The results were expressed in percentages.

Calculation of cell viability was performed in Excel. Normality of distribution of the feature by groups was estimated using the Shapiro-Wilk criterion. It was found that the distribution of features corresponds to normality, therefore, comparisons between the groups were performed using analysis of one-way ANOVA. Statistical processing and calculation of IC50 were performed in GraphPad Prism 8.0 (San Diego). Values of P < 0.05 were considered to be significant for both cytotoxicity and X-ray induced cytotoxicity of  $La_{1-x}Pr_xPO_4$  NPs. Results were presented as mean  $\pm$  SD.

#### **Results and discussion**

Transmission electron microscopy

As can be seen from the TEM images (Fig. 1), NPs with different aspect ratios (AR) were obtained: nanofibers

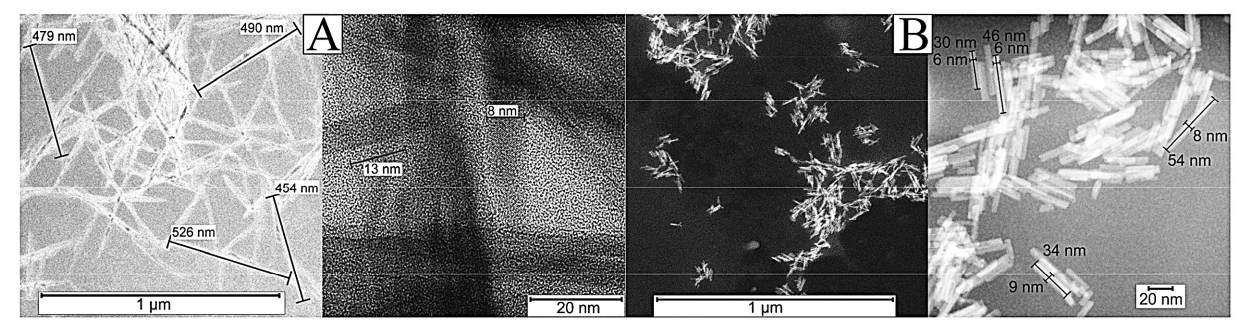


**Рис. 1.** Различные морфологии и размеры HЧ  $La_{1-x}Pr_xPO_4$ , синтезированных гидротермально-микроволновым методом (200 °C, 2 ч): А – нановолокна  $La_{0.98}Pr_{0.02}PO_4$ ; В – наностержни  $La_{0.95}Pr_{0.05}PO_4$ . **Fig. 1.** Different morphologies and sizes of  $La_{1-x}Pr_xPO_4$  NPs prepared by microwave-assisted hydrothermal method (200 °C, 2 hours): A –  $La_{0.98}Pr_{0.02}PO_4$  nanofibers; B –  $La_{0.95}Pr_{0.05}PO_4$  nanorods.

ORIGINAL ARTICLES

(nanofiber sample, AR > 30) (Fig. 1a) and nanorods (nanorod sample,  $AR \approx 5$ ) (Fig. 1b). The measured sizes of the NPs from the nanofiber sample do not exceed 600 nm in length and 15 nm in diameter, and the NPs from the nanorod sample do not exceed 80 nm in length and 10 nm in diameter. As follows from the TEM analysis, the sizes of the obtained NPs strongly depend on the synthesis conditions: pH and the ratio of excess anions. With an increase in these parameters, the sizes of the NPs decrease significantly.

X-ray excited optical luminescence spectroscopy of La, Pr PO colloidal solutions

The X-ray optical luminescence spectra in the UV-C region of the obtained colloidal solutions consist of three broad luminescence bands of the transitions 4f<sup>1</sup>5d<sup>1</sup>  $\rightarrow$   ${}^{3}H_{A'}$   ${}^{3}H_{5'}$   ${}^{3}H_{6}$  ( ${}^{3}F_{2}$ ) in Pr<sup>3+</sup> ions (Fig. 2). The noise vertical lines observed in the spectra are a consequence of the penetration of X-ray quanta into the CCD camera, which was located in the path of the X-ray tube window.

The transition from nanofibers to nanorods caused a strong weakening of the fluorescence intensity. The observed UV-C luminescence brightness is about 6.3 times higher for the nanofiber sample (Fig. 2, curve A) than that for nanorod sample (Fig. 2, curve B). For nanofibers, the intensities of long-wave transition  $(4f^15d^1 \rightarrow {}^3H_z)$ predominate, whereas for nanorods, the intensities of transitions from 4f<sup>1</sup>5d<sup>1</sup> to the levels of the ground triplet <sup>3</sup>H, are practically the same.

Intrinsic cytotoxicity of nanoparticles according to MTT

The viability of Mh22a and L929 cell cultures (Fig. 3) was assessed using the MTT assay after 24 h of incubation with La<sub>0.95</sub>Pr<sub>0.05</sub>PO<sub>4</sub> nanorod and La<sub>0.98</sub>Pr<sub>0.02</sub>PO<sub>4</sub> nanofiber samples at different concentrations of NPs (0.0625 - 4 mg/mL) in DMEM culture medium. Cytotoxicity for all samples was observed at a NPs concentration of 4 mg/mL.

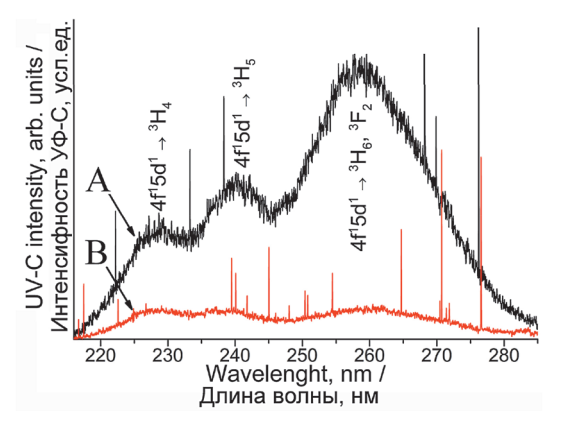
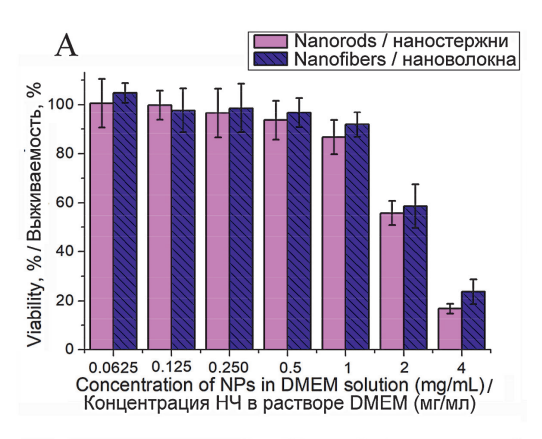


Рис. 2. УФ-С спектры рентгенолюминесценции коллоидных растворов (7 мг/мл): A – нановолокна  $La_{0.98}Pr_{0.02}PO_4$ ; B – наностержни  $La_{0.95}$   $Pr_{0.05}$   $PO_4$ . Режим работы рентгеновской трубки: ускоряющее напряжение 30 кВ, анодный ток 2,5 мА, время экспозиции 60 с.

Fig. 2. X-ray excited UV-C spectra of colloidal solutions (7 mg/ mL) samples: A -  $La_{0.98}Pr_{0.02}PO_4$  nanofibers; B -  $La_{0.98}Pr_{0.02}PO_4$ nanorods. X-ray tube operating mode: accelerating voltage 30 kV, anode current 2.5 mA, exposure time 60 s.



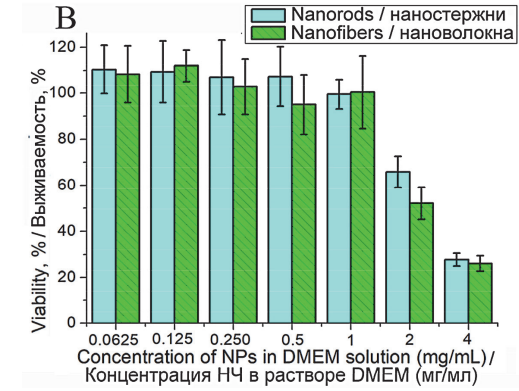


Рис. 3. Результаты МТТ анализа по выживаемости клеток Mh22a (A) и L929 (B) после 24 часов инкубации с наностержнями La $_{0.95}$ Pr $_{0.05}$ PO $_4$  (сплошные столбцы) и нановолоконами La $_{0.98}$ Pr $_{0.02}$ PO $_4$  (штрихованные столбцы) при разных концентрациях HЧ.

Fig. 3. Results of MTT assay for viability of Mh22a (A) and L929 (B) cells after 24 hours of incubation with  $La_{0.95}Pr_{0.05}P0_4$  nanorods (solid bars) and  $La_{0.98}Pr_{0.02}P0_4$  nanofibers (hatched bars) at different NPs concentrations.

At concentrations in the range of 0.0625 – 1 mg/mL, cell viability was more than 90% for both types of NPs.

For the studied samples of colloidal solutions, the calculated IC50 parameters (Table 1) indicate that they can be classified as low cytotoxic compounds for Mh22a and L929 cell cultures (according to the international standard ISO SO 10993-5:2009). As can be seen for the Mh22a cell line, the nanofiber sample has a slightly higher IC50 value than the nanorod sample. For the L929 cell line, IC50 is slightly higher for the nanorod sample. This may be due to the fact that the nanorod and nanofiber samples were treated differently at the washing stage (washings with addition of NH<sub>4</sub>OH or HNO<sub>3</sub>, respectively), which may cause different cell responses to NPs depending on the cell line. However, the observed difference in IC50 values is quite small.

Cytotoxicity after X-ray irradiation according to MTT

The X-ray irradiation modes on the cell samples were selected to cause low cell death of the control groups of Mh22a and L929 cells (about 10%) (Figs. 4A and 5A, respectively). The irradiation dose was based on previously



**Таблица 1** Л $\mathsf{Д}_{50}$  для исследованных образцов по результатам МТТ анализа

**Table 1** IC<sub>50</sub> of the studied samples according to MTT assay

Культура клеток Cell culture	Образец НЧ NPs sample	ЛД <sub>50</sub> , мг/мл IC <sub>50</sub> , mg/mL
Mh22a	La <sub>0.95</sub> Pr <sub>0.05</sub> PO <sub>4</sub> наностержни La <sub>0.95</sub> Pr <sub>0.05</sub> PO <sub>4</sub> nanorods	2.082
	La <sub>0.98</sub> Pr <sub>0.02</sub> PO <sub>4</sub> нановолокна La <sub>0.98</sub> Pr <sub>0.02</sub> PO <sub>4</sub> nanofibers	2.556
L929	La <sub>0.95</sub> Pr <sub>0.05</sub> PO <sub>4</sub> наностержни La <sub>0.95</sub> Pr <sub>0.05</sub> PO <sub>4</sub> nanorods	2.354
	La <sub>0.98</sub> Pr <sub>0.02</sub> PO <sub>4</sub> нановолокна La <sub>0.98</sub> Pr <sub>0.02</sub> PO <sub>4</sub> nanofibers	2.025

conducted experiments was 8 Gy. As an additional control, groups of Mh22a and L929 cells were irradiated with a UV lamp at 60 J/cm<sup>2</sup> for 8 min, which resulted in a strong decrease in viability (74% and 68%, respectively) (Fig. 4A and 5A, respectively).

The results of the MTT assay for the X-ray-induced cytotoxicity of the studied colloidal solutions on the viability of Mh22a cells demonstrate a significant decrease in viability only in the group of cells incubated with the sample of La<sub>0.98</sub>Pr<sub>0.02</sub>PO<sub>4</sub> nanofibers at a concentration of 2 mg/mL. In this case, the cell viability decreased by 28%

and 25% (for irradiation modes 1 and 2, respectively) compared to the group of cells incubated with the same conditions without exposure to X-rays (Fig. 4E). For the group of L929 cells incubated with the sample of La<sub>0.98</sub>Pr<sub>0.02</sub>PO<sub>4</sub> nanofibers at a NPs concentration of 2 mg/mL, the cell viability decreased by 24% and 17% (for irradiation modes 1 and 2, respectively) compared to the group of cells incubated with the same conditions without exposure to X-rays (Fig. 4J). Thus, the results of the MTT assay after the addition of NPs and X-ray irradiation showed a slightly stronger effect on Mh22a cancer cells than on L929 healthy fibroblasts. Unfortunately, MTT results for X-ray irradiation of both cell cultures incubated with 1 and 2 mg/mL of  $La_{0.95}Pr_{0.05}PO_4$  nanorod or 1 mg/mL of La<sub>0.98</sub>Pr<sub>0.02</sub>PO<sub>4</sub> nanofiber samples showed little change in cell viability compared to incubation with the same NPs at the same concentrations without X-ray irradiation (Figs. 4B-D and G-I).

Study of the type of cell death according to fluorescence microscopy

To study the type of cytotoxicity under various influences, the double staining method with fluorescent dyes of acridine orange (AO) and propidium iodide (PI) with the subsequent fluorescence microscopy and morphological analysis were performed. The selected control groups of Mh22a and L929 cells from previous experiments were studied: untreated, treated with X-ray in mode 1 and mode 2, UV irradiated, incubated with 2 mg/mL of the  $La_{0.95}Pr_{0.05}PO_4$  nanorod sample without and with X-ray treatment in mode 1 and mode 2, incubated with 2 mg/mL of the  $La_{0.98}Pr_{0.02}PO_4$  nanofiber sample without

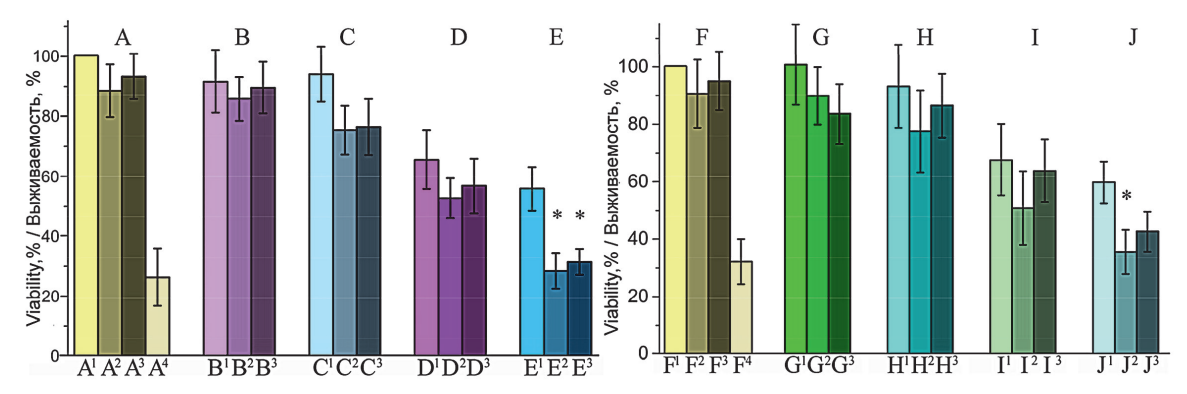


**Рис. 4.** Результаты МТТ теста по эффекту цитотоксичности на клетки Mh22a (A-E) и L929 (F-J) при различных воздействиях с последующей инкубацией в течении 24 ч. Группы столбцов соответствуют различным контрольным выборкам: А и F — отдельные эффекты: контрольные клетки ( $A^1$ ,  $F^1$ ), клетки облученные рентгеном в режиме 1 ( $A^2$ ,  $F^2$ ) и режиме 2 ( $A^3$ ,  $A^3$ ), клетки облученные УФ лампой ( $A^4$ ,  $A^4$ ); В и G — образец наностержней La<sub>0.95</sub>Pr<sub>0.05</sub>PO<sub>4</sub> (1 мг/мл) без облучения ( $A^1$ ,  $A^2$ ) и с облучением рентгеном в режиме 1 ( $A^2$ ,  $A^2$ ) и режиме 2 ( $A^3$ ,  $A^3$ ); С и H — образец нановолокон La<sub>0.98</sub>Pr<sub>0.02</sub>PO<sub>4</sub> (1 мг/мл) без облучения ( $A^2$ ,  $A^2$ ) и режиме 2 ( $A^3$ ,  $A^3$ ); С и H — образец наностержней La<sub>0.95</sub>Pr<sub>0.05</sub>PO<sub>4</sub> (2 мг/мл) без облучения ( $A^2$ ,  $A^2$ ) и режиме 2 ( $A^3$ ,  $A^3$ ); Е и J — образец нановолокон La<sub>0.98</sub>Pr<sub>0.02</sub>PO<sub>4</sub> (2 мг/мл) без облучения ( $A^2$ ,  $A^3$ ) и с облучением рентгеном в режиме 1 ( $A^2$ ,  $A^2$ ) и режиме 2 ( $A^3$ ,  $A^3$ ); Е и J — образец нановолокон La<sub>0.98</sub>Pr<sub>0.02</sub>PO<sub>4</sub> (2 мг/мл) без облучения ( $A^3$ ,  $A^3$ ) и с облучением рентгеном в режиме 1 ( $A^3$ ,  $A^3$ ) и режиме 2 ( $A^3$ ,  $A^3$ , A

**Fig. 4.** MTT assay results on cytotoxicity effect on Mh22a (A-E) and L929 (F-J) cells under the influence of various treatments followed by incubation for 24 hours. The groups of columns correspond to the different control groups: A – individual effects: control cells (A¹, F¹), cells treated with X-ray mode 1 (A², F²) and mode 2 (A³, F³), cells irradiated with UV lamp (A⁴, F⁴); B – La $_{0.95}$ Pr $_{0.05}$ PO $_4$  nanorod sample (1 mg/mL) without (B¹, G¹) and with X-ray treatment in mode 1 (B², G²) and mode 2 (B³, G³); C and H – La $_{0.95}$ Pr $_{0.02}$ PO $_4$  nanorod sample (1 mg/mL) without (C¹, H¹) and with X-ray treatment in mode 1 (C², H²) and 2 mode (C³, H³); D and I – La $_{0.95}$ Pr $_{0.05}$ PO $_4$  nanorod sample (2 mg/mL) without (D¹, I¹) and with X-ray treatment in mode 1 (D², I²) and mode 2 (D³, I³); E and J – La $_{0.98}$ Pr $_{0.02}$ PO $_4$  nanofiber sample (2 mg/mL) without (E¹, J¹) and with X-ray treatment in mode 1 (E², J²) and mode 2 (E³, J³). \* – P < 0.05



and with treatment with X-ray in mode 1 and mode 2 (see caption to Fig. 4A, D, E, F, I, J). The analysis of the number of viable (VC), apoptotic (AC) and necrotic (NC) cells was carried out according to their morphological features described in the in vitro study methodology.

The untreated groups of Mh22a and L929 cells had an intact membrane with uniform green staining of the cytoplasm and nucleus (Fig. 5A). In addition, spotted local orange fluorescence, which is more pronounced for Mh22a cells is characteristic of AO associated with active lysosomes or acidic cellular vesicles [14, 15]. The exposure to X-rays at a dose of 8 Gray in mode 1 and 2 modes did not lead to noticeable morphological changes in both cell

lines (Fig. 5B and C). Exposure of Mh22a and L929 to UV irradiation caused a strong change in cell morphology (Fig. 5D) indicating significant cell death with signs of apoptosis. Most Mh22a cells exposed to UV had disrupted membranes and a rounded shape with no evidence of active lysosomes, and their nuclei were stained orange (Fig. 5D, left side). However, in the case of L929, completely green cells with apoptotic bodies around them were observed (Fig. 5D, right side). This difference may be due to different kinetics of apoptosis depending on the cell line.

Images of Mh22a cells incubated with the nanorod and nanofiber samples without exposure to X-rays (Fig. 5E and F,

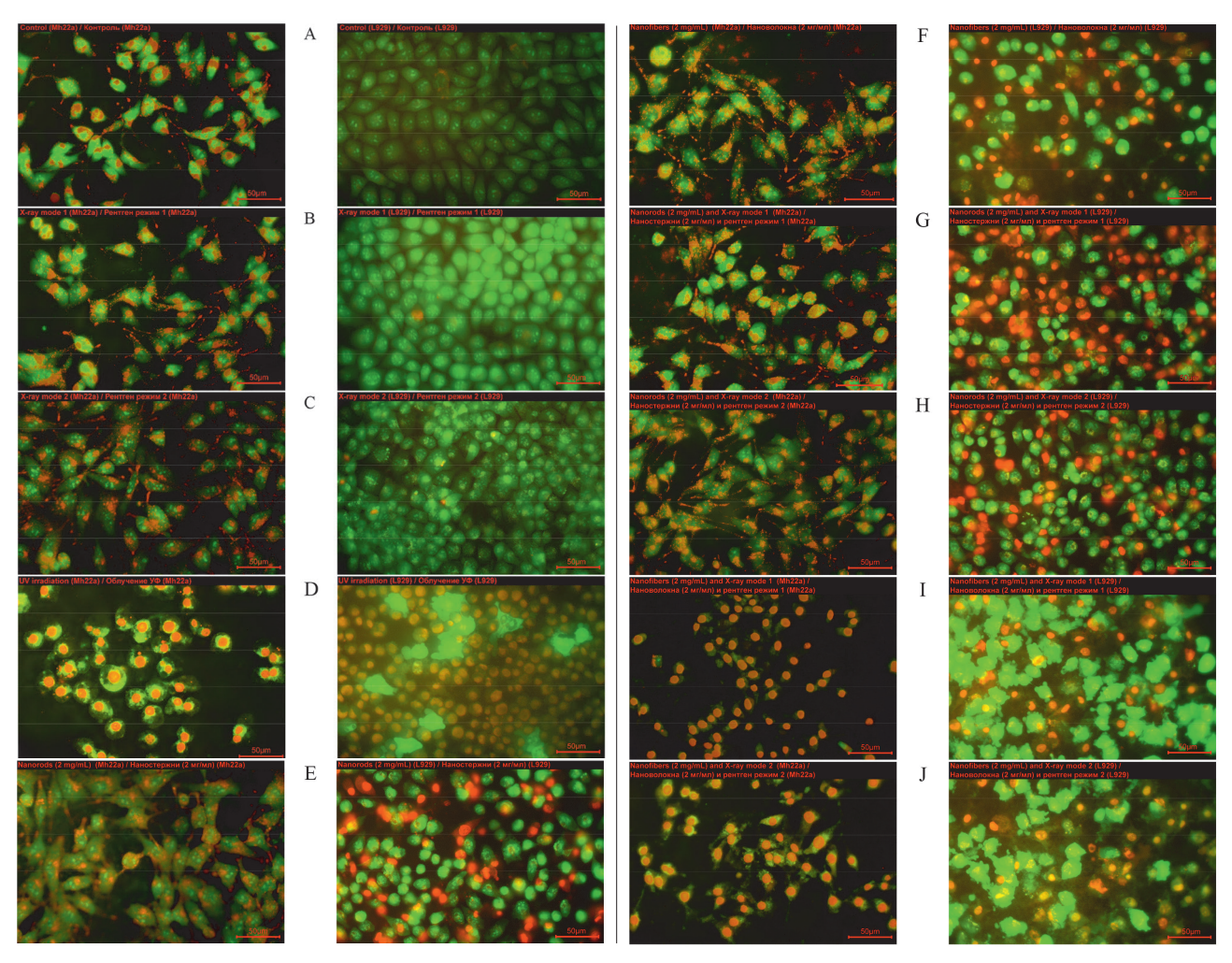


**Рис. 5.** Флуоресцентные изображения различных групп клеток Mh22a (слева) и L929 (справа) окрашенных акридиновым оранжевым и пропидий йодидом (увеличение:  $\times$ 400). А – контрольная группа (без дополнительных воздействий); В – облучение рентгеном в режиме 1; С – облучение рентгеном в режиме 2; D – облучение УФ лампой; Е – инкубация с 2 мг/мл наностержней La $_{0.95}$ Pr $_{0.05}$ PO $_4$ ; F – инкубация с 2 мг/мл нановолокон La $_{0.98}$ Pr $_{0.02}$ PO $_4$ ; G – инкубация с 2 мг/мл наностержней La $_{0.95}$ Pr $_{0.05}$ PO $_4$  и облучение рентгеном в режиме 1; H – инкубация с 2 мг/мл нановолокон La $_{0.98}$ Pr $_{0.02}$ PO $_4$  и облучение рентгеном в режиме 2; I – инкубация с 2 мг/мл нановолокон La $_{0.98}$ Pr $_{0.02}$ PO $_4$  и облучение рентгеном в режиме 2, и облучение рентгеном в режиме 2, и облучение рентгеном в режиме 2.

Fig. 5. Fluorescence images of different groups of Mh22a (left) and L929 (right) cells stained with AO and PI dyes (magnification:  $\times 400$ ). A – control cells (untreated); B – irradiation with X-ray in mode 1; C – irradiation with X-ray in mode 2; D – irradiation with UV; E – incubation with 2 mg/mL of La<sub>0.98</sub>Pr<sub>0.05</sub>PO<sub>4</sub> nanorods; F – incubation with 2 mg/mL of La<sub>0.98</sub>Pr<sub>0.05</sub>PO<sub>4</sub> nanorods and irradiation with X-ray in mode 1; H – incubation with 2 mg/mL of La<sub>0.95</sub>Pr<sub>0.05</sub>PO<sub>4</sub> nanorods and irradiation with X-ray in mode 2; I – incubation with 2 mg/mL of La<sub>0.98</sub>Pr<sub>0.02</sub>PO<sub>4</sub> nanorods and irradiation with X-ray in mode 2; I – incubation with X-ray in mode 2.

left side, respectively) showed signs of apoptosis and, to a lesser extent, signs of necrosis, but a fairly large number of viable cells were preserved. Also, of note is the increase in spotted local orange fluorescence, indicating higher lysosomal activity of cells, possibly caused by oxidative stress induced by NPs). In fact, NPs containing REIs may exhibit catalytic properties and participate in oxidationreduction reactions, causing cell death [16]. However, the majority of cells were uniformly stained green by AO, indicating the integrity of the cell membranes. For L929 cells incubated with the nanorod sample (Fig. 5E, right side), a higher number of necrotic cells with red staining of the nucleus and cytoplasm were observed. However, the response of L929 cells to incubation with the nanofiber sample (Fig. 5F, right side) resulted in an increase in the number of AC with orange staining of nuclei or green staining with apoptotic bodies around them.

Exposure to X-rays (in both irradiation modes) of Mh22a cells incubated with the nanorod sample caused rounding of some of the cells, single apoptotic and necrotic cells were also observed (Fig. 5G, H, left side). For L929 cells incubated with the nanorod sample and irradiated with X-rays (in both modes), slightly higher numbers of necrotic cells were observed (Fig. 5G, H, right side). In contrast, in the groups of Mh22a cells incubated with 2 mg/mL nanofiber and treated with X-rays in mode 1 and 2 (Fig. 5I and J, left side), a decrease in the number of VC and a significant increase in the number of AC was observed. The apoptotic Mh22a cells were determined by the shrinkage and rounding of cells and intense orange fluorescence of the nucleus, which is caused by the destruction of the

native DNA structure and the binding of DNA fragments to AO dye. Single necrotic Mh22a cells, appearing as red nucleus, were also seen in this case. Similar visual effects were observed for L929 cells incubated with the nanofiber sample and treated with X-rays in mode 1 and 2 (Fig. 5I and J, right side). However, in the case of L929 cells, more cells with apoptotic bodies around them were observed, which again may be due to different apoptosis kinetics depending on the cell line.

Based on morphological analysis of fluorescence microscope images, statistics of the distribution of viable (VC), apoptotic (AC) and necrotic (NC) cells were obtained for Mh22a and L929 cell cultures (Fig. 6A and B, respectively). In general, the pattern for X-ray and UV (Fig. 6A<sup>2</sup>-A<sup>4</sup>, B<sup>2</sup>-B<sup>4</sup>) exposure is similar for both types of cell cultures and in good agreement with MTT results (Fig. 4A, F). However, for Mh22a cells irradiated with a UV lamp (Fig. 6A4), an almost complete absence of VC was observed, which differs from the MTT results (Fig. 4A). The obtained statistics on VC after incubation of cells with NPs with or without subsequent X-ray irradiation (Fig. 6A<sup>5</sup>-A<sup>10</sup> and B<sup>5</sup>-B<sup>10</sup>) are also in good agreement with MTT data (Fig. 4D, E, I, J). Additionally, control groups of Mh22a cells incubated with NPs solutions at a concentration of 2 mg/mL demonstrated higher cell survival according to fluorescence microscopy data (Fig. 6A) compared to the MTT assay (Fig. 4D, E). The observed differences in AC/ NC ratio between the UV irradiated control groups of the Mh22a and L929 cell lines (Fig. A<sup>4</sup> and B<sup>4</sup>, respectively) are likely due to the faster kinetics of apoptosis for L929 cells, making them less distinguishable from necrotic cells.

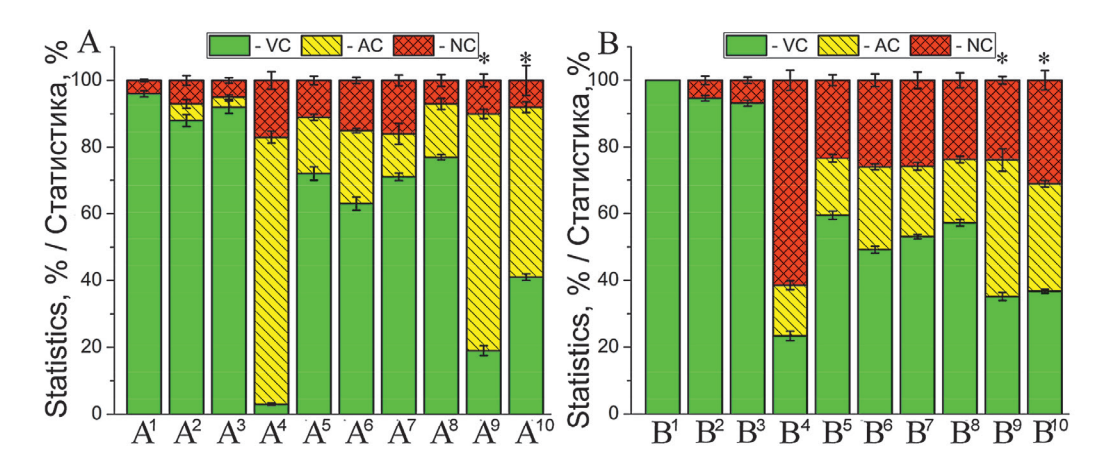


**Рис. 6.** Морфологический анализ изображений с флуоресцентного микроскопа живых (VC), апоптотических (AC) и мертвых (NC) клеток для A-Mh22a и B-L929 клеточных культур при различных воздействиях: клетки без дополнительных воздействий ( $A^1$ ,  $B^1$ ), облучение рентгеном в режиме 1 ( $A^2$ ,  $B^2$ ) и режиме 2 ( $A^3$ ,  $B^3$ ), облучение  $Y\Phi$  лампой ( $A^4$ ,  $B^4$ ), инкубация клеток с 2 мг/мл наностержней  $La_{0.95}Pr_{0.05}PO_4$  без облучения ( $A^5$ ,  $B^5$ ) и с облучением рентгеном в режиме 1 ( $A^6$ ,  $B^6$ ) и режиме 2 ( $A^7$ ,  $B^7$ ), инкубация клеток с 2 мг/мл нановолокон  $La_{0.98}Pr_{0.02}PO_4$  без облучения ( $A^8$ ,  $B^8$ ) и с облучением рентгеном в режиме 1 ( $A^9$ ,  $A^9$ ) и режиме 1 ( $A^9$ ) и режиме 1 и режиме 1 ( $A^9$ ) и режиме 1 ( $A^9$ ) и режиме 1 и режиме 1

**Fig. 6.** Morphological analysis of fluorescence microscope images of viable (VC), apoptotic (AC) and necrotic and death (NC) cells for A – Mh22a and B – L929 cell cultures under various influences: untreated cells ( $A^1$ ,  $B^1$ ), X-ray irradiation in mode 1 ( $A^2$ ,  $B^2$ ) and mode 2 ( $A^3$ ,  $B^3$ ), UV irradiation ( $A^4$ ,  $A^4$ ), incubation with 2 mg/mL of the La<sub>0.95</sub>Pr<sub>0.05</sub>PO<sub>4</sub> nanorod sample without ( $A^5$ ,  $A^5$ ) and with X-ray irradiation in mode 1 ( $A^6$ ,  $A^6$ ) and mode 2 ( $A^7$ ,  $A^7$ ), incubation with 2 mg/mL of the La<sub>0.98</sub>Pr<sub>0.02</sub>PO<sub>4</sub> nanofiber sample without ( $A^8$ ,  $A^8$ ) X-ray and with X-ray irradiation in mode 1 ( $A^9$ ,  $A^9$ ) and mode 2 ( $A^{10}$ ,  $A^{10}$ ). \* – P < 0.05

The apoptotic cycle of Mh22a cells probably takes longer, resulting in better distinguishability and an increased AC/NC ratio.

The obtained statistics of morphological distributions (Fig. 6) indicated a significant decrease in the survival rate of the studied cell lines due to apoptosis after incubation with the La<sub>0.98</sub>Pr<sub>0.02</sub>PO<sub>4</sub> nanofiber sample (2 mg/mL) and irradiation with X-rays. This effect becomes more noticeable when the cells are irradiated with X-rays in mode 1 than in mode 2, which is consistent with the MTT assay results (Fig. 4). In addition, the microscopy results indicated a higher sensitivity of Mh22a cancer cells to the studied effects compared to L929, which is also in agreement with the MTT assay results (Fig. 4). Unfortunately, the obtained statistics on the effect of the La<sub>0.95</sub>Pr<sub>0.05</sub>PO<sub>4</sub> nanorod sample (2 mg/mL) and X-ray irradiation showed that the effect is practically absent for both cell cultures (Fig. 6A<sup>5</sup>-A<sup>7</sup> and B<sup>5</sup>-B<sup>7</sup>), which is also in full agreement with the results of the MTT assay (Fig. 4D, I).

Presumably, the decrease in viability of Mh22a and L929 cells was influenced by UV-C generated by nanofiber sample under the influence of X-rays, since in this case cell apoptosis is observed. At the same time, other effects acting on the cell under the influence of NPs reacting with X-rays are also possible, for example, the formation of secondary electrons by NPs or heating of NPs, which can also lead to the deactivation of irradiated cells. The mentioned catalytic activity of NPs doped with REI can also enhance the effect of X-rays. Some studies also report increased cytotoxicity due to apoptosis of NPs with a positively charged surface [17, 18]. Thus, part of the intrinsic cytotoxicity of nanofiber sample may be due to the positively charged adsorption and diffusion layers after washing with HNO<sub>3</sub> solution. In addition, nanorods obtained in an alkaline medium with ammonium tartrate solution can desorb molecules and ions under the influence of X-rays, such as hydroxyl groups, ammonia ions or tartaric acid residues, which can also lead to additional cell death by necrosis. However, despite this, we believe that the main cytotoxic effect was caused by UV-C radiation, since in this case the morphology of the cells is similar to cells irradiated with a UV lamp. Moreover, in [4] it was shown that LuPO, NPs without an activator have virtually no effect on X-ray-induced cytotoxicity relative to LuPO<sub>4</sub>:Pr<sup>3+</sup> NPs.

It should also be noted that for the successful use of NPs in cancer therapy it is necessary to reduce the concentration of the applied NPs and reduce the effect of intrinsic necrosis. Therefore, more experiments on optimization of synthesis and washing procedure of NPs and their surface functionalization are required to further improve their therapeutic potential. In addition, more extensive studies are needed to examine the mechanisms of cytotoxicity by which NPs act on different cell types under different X-ray irradiation regimens.

### **Conclusion**

Two colloidal solutions of La<sub>1-x</sub>Pr<sub>x</sub>PO<sub>4</sub> NPs with nanofiber (length & diameter not larger than 600 & 15 nm, respectively) and nanorod (length & diameter not larger than 80 & 10 nm, respectively) morphologies were prepared by the hydrothermal microwave-assisted method. Measurement of X-ray excited optical luminescence spectra in the UV-C range from the obtained colloidal solutions showed a large difference in brightness: for larger NPs, the brightness was 6.3 times higher.

According to the MTT assay, the prepared colloidal solutions were classified as low-cytotoxic compounds (IC50 > 2 mg/mL) for Mh22a and L929 cell lines. A significant decrease in cell viability under the influence of X-rays was achieved only for groups of cells incubated with 2 mg/mL of colloidal solutions consisting of NPs having nanofiber morphology with 2 mole-% doping of Pr<sup>3+</sup> ions. After X-ray irradiation, groups of Mh22a and L929 cells incubated with colloidal solutions of La<sub>0.08</sub>Pr<sub>0.02</sub>PO<sub>4</sub> nanofiber NPs showed pronounced cell apoptosis, which may indicate the successful effect of UV-C quanta generated under the influence of X-rays on controlled cell death. According to MTT assay and fluorescence microscopy, the effect of X-ray-induced NPs cytotoxicity is more pronounced for cancer cells and increases with decreasing accelerating voltage of the X-ray tube. Therefore, the potential for therapeutic use of La, Pr.PO, NPs has been shown. Unfortunately, the use of NPs with nanorod morphology did not significantly enhance the X-ray irradiation effect, indicating the need to increase their X-ray excited UV-C brightness. Fluorescence microscopy showed that the intrinsic and X-ray induced cytotoxicity of La<sub>0.95</sub>Pr<sub>0.05</sub>PO<sub>4</sub> colloidal solutions consisting of NPs with nanorod morphology is mostly due to cell necrosis for L929 and Mh22a cell lines. Further research is needed to clarify the cause and type of cell death for various cell cultures incubated with La,\_\_,Pr,PO, NPs and irradiated with X-rays. For medical application of La<sub>1-x</sub>Pr<sub>x</sub>PO<sub>4</sub> NPs, it is still necessary to increase their UV-C luminescence intensity under X-ray excitation and modify their surface, which should lead to an increase in X-ray induced cytotoxicity, a decrease in the practical concentration of the NPs in colloids, and a decrease in intrinsic cytotoxicity.

# **Acknowledgments**

V.Y.G., S.G.O., O.E.O. and S.A.T. are grateful for a support of the Russian Science Foundation (grant number 22-22-00998 for small scientific groups). Authors are grateful to Nikolay Pyatayev for organizing the in vitro studies. G.I.A., A.-k.A.A.M., C.R.A. and Y.D.E. are grateful to Nikolay A. Pyatayev and Mikhail N. Zharkov for their help in writing the text of the in vitro results analysis and formulating the conclusions to them.

# **REFERENCES**

- Miwa S., Yano S., Hiroshima Y., Tome Y., Uehara F., Mii S., Efimova E.V., Kimura H., Hayashi K., Tsuchiya H., Hoffman R.M. Imaging UVC-induced DNA damage response in models of minimal cancer. *J. Cell. Biochem*, 2013, vol. 114(11), pp. 2493-2499.
- Müller M., Espinoza S., Jüstel T., Held K.D., Anderson R.R., Purschke M. UVC-Emitting LuPO<sub>4</sub>:Pr<sup>3+</sup> Nanoparticles Decrease Radiation Resistance of Hypoxic Cancer Cells. *Radiat*. Res, 2020, vol. 193(1), pp. 82-87
- Squillante M. R., Jüstel T., Anderson R.R., Brecher C., Chartier D., Christian J.F., Cicchetti N., Espinoza S., McAdams D.R., Müller M., Tornifoglio B., Wang Y., Purschke M. Fabrication and characterization of UV-emitting nanoparticles as novel radiation sensitizers targeting hypoxic tumor cells. Opt. Mater, 2018, vol. 80, pp. 197-202.
- Espinoza S., Müller M., Jenneboer H., Peulen L., Bradley T., Purschke M., Haase M., Rahmanzadeh R., Jüstel T. Characterization of Micro- and Nanoscale LuPO<sub>4</sub>·Pr<sup>3+</sup>, Nd<sup>3+</sup> with Strong UV-C Emission to Reduce X-Ray Doses in Radiation Therapy. *Part. Part. Syst. Charact*, 2019, vol. 36(10), pp. 1900280.
- Espinoza S., Volhard M.-F., Kätker H., Jenneboer H., Uckelmann A., Haase M., Müller M., Purschke M., Jüstel T. Deep Ultraviolet Emitting Scintillators for Biomedical Applications: The Hard Way of Downsizing LuPO<sub>4</sub>:Pr<sup>3+</sup>. Part. Part. Syst. Charact, 2018, vol. 35(12), pp. 1800282.
- Tran T. A., Kappelhoff J., Jüstel T., Anderson R.R., Purschke M.U. V emitting nanoparticles enhance the effect of ionizing radiation in 3D lung cancer spheroids. *Int. J. Radiat. Biol*, 2022, vol. 98(9), pp. 1484-1494.
- Malyy T.S., Vistovskyy V.V., Khapko Z.A., Pushak A.S., Mitina N.E., Zaichenko A.S., Gektin A.V., Voloshinovskii A.S. Recombination luminescence of LaPO<sub>4</sub>-Eu and LaPO<sub>4</sub>-Pr nanoparticles. *J. Appl. Phys*, 2013, vol. 113(22), pp. 224305.
- Srivastava A.M., Setlur A.A., Comanzo H.A., Beers W.W., Happek U., Schmidt P. The influence of the Pr<sup>3+</sup> <sup>4</sup>f<sup>15</sup>d¹ configuration on the ¹S<sub>0</sub> emission efficiency and lifetime in LaPO<sub>4</sub>. Opt. Mater, 2011, vol. 33(3), pp. 292-298.
- Okamoto S., Uchino R., Kobayashi K., Yamamoto H. Luminescent properties of Pr<sup>3+</sup>-sensitized LaPO<sub>4</sub>:Gd<sup>3+</sup> ultraviolet-B phosphor under vacuum-ultraviolet light excitation. *J. Appl. Phys*, 2009, vol. 106(1), pp. 013522.
- Srivastava A.M. Aspects of Pr<sup>3+</sup> luminescence in solids. *J. Lumin*, 2016, vol. 169(B), pp. 445-449.
- Bagatur'yants A.A., Iskandarova I.M., Knizhnik A.A., Mironov V.S., Potapkin B.V., Srivastava A.M., Sommerer T.J. Energy level structure of <sup>4</sup>f<sup>5</sup>d states and the Stokes shift In LaPO<sub>4</sub>:Pr<sup>3+</sup>: A theoretical study. *Phys. Rev. B.*, 2008, vol. 78(16), pp. 165125.
- Hilario E.G., Rodrigues L.C.V., Caiut J.M.A. Spectroscopic study of the 4f5d transitions of LaPO4 doped with Pr<sup>3+</sup> or co-doped with Pr<sup>3+</sup> and Gd<sup>3+</sup> in the vacuum ultra violet region. *Nanotechnology*, 2022, vol. 33, pp. 305703. https://doi.org/10.1088/1361-6528/ ac6679
- McGahon A.J., Martin S.J., Bissonnette R.P., Mahboubi A., Shi Y., Mogil R.J., Nishioka W.K., Green D.R. The end of the (cell) line: methods for the study of apoptosis in vitro. *Methods Cell Biol*, 1995, vol. 46, pp. 153-185.
- Kusuzaki K., Murata H., Matsubara T., Satonaka H., Wakabayashi T., Matsumine A., Uchida A. Review. Acridine orange could be an innovative anticancer agent under photon energy. *In Vivo*, 2007, vol. 21(2), pp. 205-214.
- Qian H., Chao X., Williams J., Fulte S., Li T., Yang L., Ding W. X. Autophagy in liver diseases: A review. Mol Aspects Med, 2021, vol. 82, pp. 100973
- Xu C. and Qu X. Cerium oxide nanoparticle: a remarkably versatile rare earth nanomaterial for biological applications. NPG Asia Mater, 2014, vol. 6(3), pp. e90-e90.
- Goodman C. M., McCusker C. D., Yilmaz T., Rotello V.M. Toxicity of gold nanoparticles functionalized with cationic and anionic side chains. *Bioconjugate Chem*, 2004, vol. 15(4), pp. 897-900.
- Schaeublin N.M., Braydich-Stolle L.K., Schrand A.M., Miller J.M., Hutchison J., Schlager J.J., Hussain S.M. Surface charge of gold nanoparticles mediates mechanism of toxicity. *Nanoscale*, 2011, vol. 3(2), pp. 410-420.

#### **ЛИТЕРАТУРА**

- Miwa S., Yano S., Hiroshima Y., Tome Y., Uehara F., Mii S., Efimova E.V., Kimura H., Hayashi K., Tsuchiya H., Hoffman R.M. Imaging UVC-induced DNA damage response in models of minimal cancer // J. Cell. Biochem. – 2013. – Vol. 114(11). – P. 2493-2499.
- Müller M., Espinoza S., Jüstel T., Held K.D., Anderson R.R., Purschke M. UVC-Emitting LuPO<sub>4</sub>:Pr<sup>3+</sup> Nanoparticles Decrease Radiation Resistance of Hypoxic Cancer Cells // Radiat. Res. – 2020. – Vol. 193(1). – P. 82-87.
- Squillante M. R., Jüstel T., Anderson R.R., Brecher C., Chartier D., Christian J.F., Cicchetti N., Espinoza S., McAdams D.R., Müller M., Tornifoglio B., Wang Y., Purschke M. Fabrication and characterization of UV-emitting nanoparticles as novel radiation sensitizers targeting hypoxic tumor cells // Opt. Mater. 2018. Vol. 80. P. 197-202.
- Espinoza S., Müller M., Jenneboer H., Peulen L., Bradley T., Purschke M., Haase M., Rahmanzadeh R., Jüstel T. Characterization of Microand Nanoscale LuPO<sub>4</sub>:Pr³+, Nd³+ with Strong UV-C Emission to Reduce X-Ray Doses in Radiation Therapy // Part. Part. Syst. Charact. 2019. Vol. 36(10). P. 1900280.
- Espinoza S., Volhard M.-F., Kätker H., Jenneboer H., Uckelmann A., Haase M., Müller M., Purschke M., Jüstel T. Deep Ultraviolet Emitting Scintillators for Biomedical Applications: The Hard Way of Downsizing LuPO<sub>4</sub>:Pr<sup>3+</sup> // Part. Part. Syst. Charact. – 2018. – Vol. 35(12). – P. 1800282.
- Tran T. A., Kappelhoff J., Jüstel T., Anderson R.R., Purschke M.U. V emitting nanoparticles enhance the effect of ionizing radiation in 3D lung cancer spheroids // Int. J. Radiat. Biol. – 2022. – Vol. 98(9). – P. 1484-1494.
- Malyy T.S., Vistovskyy V.V., Khapko Z.A., Pushak A.S., Mitina N.E., Zaichenko A.S., Gektin A.V., Voloshinovskii A.S. Recombination luminescence of LaPO<sub>4</sub>-Eu and LaPO<sub>4</sub>-Pr nanoparticles // J. Appl. Phys. – 2013. – Vol. 113(22). – P. 224305.
- 8. Srivastava A.M., Setlur A.A., Comanzo H.A., Beers W.W., Happek U., Schmidt P. The influence of the  $Pr^{3+}$  4f¹5d¹ configuration on the  $^1S_0$  emission efficiency and lifetime in  $LaPO_4$  // Opt. Mater. 2011. Vol. 33(3). P. 292-298.
- Okamoto S., Uchino R., Kobayashi K., Yamamoto H. Luminescent properties of Pr<sup>3+</sup> -sensitized LaPO<sub>4</sub>:Gd<sup>3+</sup> ultraviolet-B phosphor under vacuum-ultraviolet light excitation // J. Appl. Phys. – 2009. – Vol. 106(1). – P. 013522.
- 10. Srivastava A.M. Aspects of  $Pr^{3+}$  luminescence in solids // J. Lumin. -2016.-169(B).-P.445-449.
- Bagatur'yants A.A., Iskandarova I.M., Knizhnik A.A., Mironov V.S., Potapkin B.V., Srivastava A.M., Sommerer T.J. Energy level structure of <sup>4</sup>5<sup>3</sup>d states and the Stokes shift In LaPO<sub>4</sub>:Pr<sup>3+</sup>: A theoretical study // Phys. Rev. B. – 2008. – Vol. 78(16). – P. 165125.
- Hilario E.G., Rodrigues L.C.V., Caiut J.M.A. Spectroscopic study of the <sup>4</sup>f<sup>5</sup>d transitions of LaPO<sub>4</sub> doped with Pr<sup>3+</sup> or co-doped with Pr<sup>3+</sup> and Gd<sup>3+</sup> in the vacuum ultra violet region // Nanotechnology. – 2022. – Vol. 33. – P. 305703.
- 13. McGahon A.J., Martin S.J., Bissonnette R.P., Mahboubi A., Shi Y., Mogil R.J., Nishioka W.K., Green D.R. The end of the (cell) line: methods for the study of apoptosis *in vitro* // Methods Cell Biol. 1995. Vol. 46. P. 153-185.
- 14. Kusuzaki K., Murata H., Matsubara T., Satonaka H., Wakabayashi T., Matsumine A., Uchida A. Review. Acridine orange could be an innovative anticancer agent under photon energy // In Vivo. 2007. Vol. 21(2). P. 205-214.
- Qian H., Chao X., Williams J., Fulte S., Li T., Yang L., Ding W. X. Autophagy in liver diseases: A review // Mol Aspects Med. – 2021. – Vol. 82. – P. 100973.
- Xu C. and Qu X. Cerium oxide nanoparticle: a remarkably versatile rare earth nanomaterial for biological applications // NPG Asia Mater. – 2014. – Vol. 6(3). – P. e90-e90.
- Goodman C. M., McCusker C. D., Yilmaz T., Rotello V.M. Toxicity of gold nanoparticles functionalized with cationic and anionic side chains // Bioconjugate Chem. – 2004. – Vol. 15(4). – P. 897-900.
- Schaeublin N.M., Braydich-Stolle L.K., Schrand A.M., Miller J.M., Hutchison J., Schlager J.J., Hussain S.M. Surface charge of gold nanoparticles mediates mechanism of toxicity // Nanoscale. – 2011. – Vol. 3(2). – P. 410-420.